Electronic Supplementary Material (ESI) for Dalton Transactions.

Pushing the photodelivery of nitric oxide to the visible: Are {FeNO}^{7} complexes good candidates?

Natalia Levin;[†] Julián Perdoménico;[†] Eckhard Bill;[‡] Thomas Weyhermüller;[‡] Leonardo D. Slep*,[†]

[†] Departamento de Química Inorgánica, Analítica y Química Física, Facultad de Ciencias Exactas y Naturales, and INQUIMAE, Universidad de Buenos Aires – CONICET, Pabellón 2, 3er piso, Ciudad Universitaria, C1428EHA, Ciudad Autónoma de Buenos Aires, Argentina.

[‡] Max-Planck-Institut für Chemische Energiekonversion, Stiftstraße 34-36, D-45470, Mülheim an der Ruhr, Germany.

Characterization of Me[9]aneN$_3$

Figure S1. ^{1}H-NMR spectrum of Me[9]aneN$_3$ in CDCl$_3$. a) δ = 2.35 ppm, 3H, b) δ = 2.48 ppm, 4H, c, d) δ = 2.35 ppm, 7.9 H.

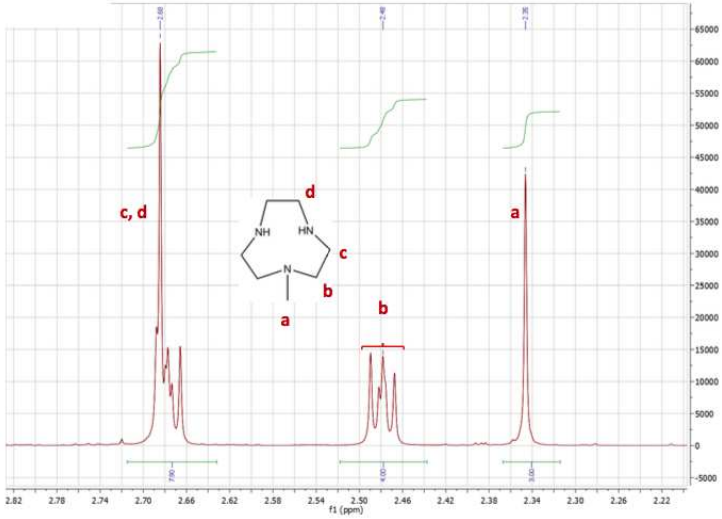

Figure S2. DEPT ^{13}C-NMR spectrum of Me[9]aneN$_3$ in CDCl$_3$. α) δ = 45.11 ppm β) δ = 54,42 ppm, γ, ε) δ = 45.99, 46.35.

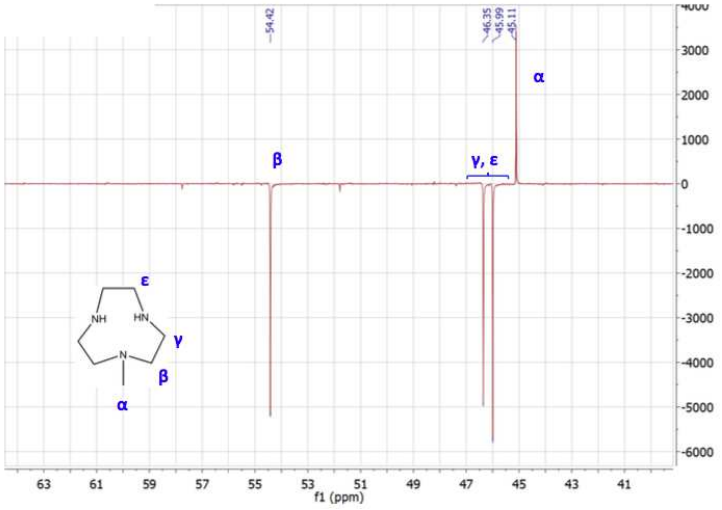

Characterization of $(CH_2Py)_2Me[9]aneN_3$

Figure S3. DEPT ^{13}C-NMR spectrum of $(CH_2Py)_2Me[9]aneN_3$ in CD_3CN. δ = 47.13, 56.91, 58.33, 59.18, 65.78, 123.17, 124.49, 137.57, 150.02 ppm. * corresponds to $CHCl_3$ from the extraction procedure.

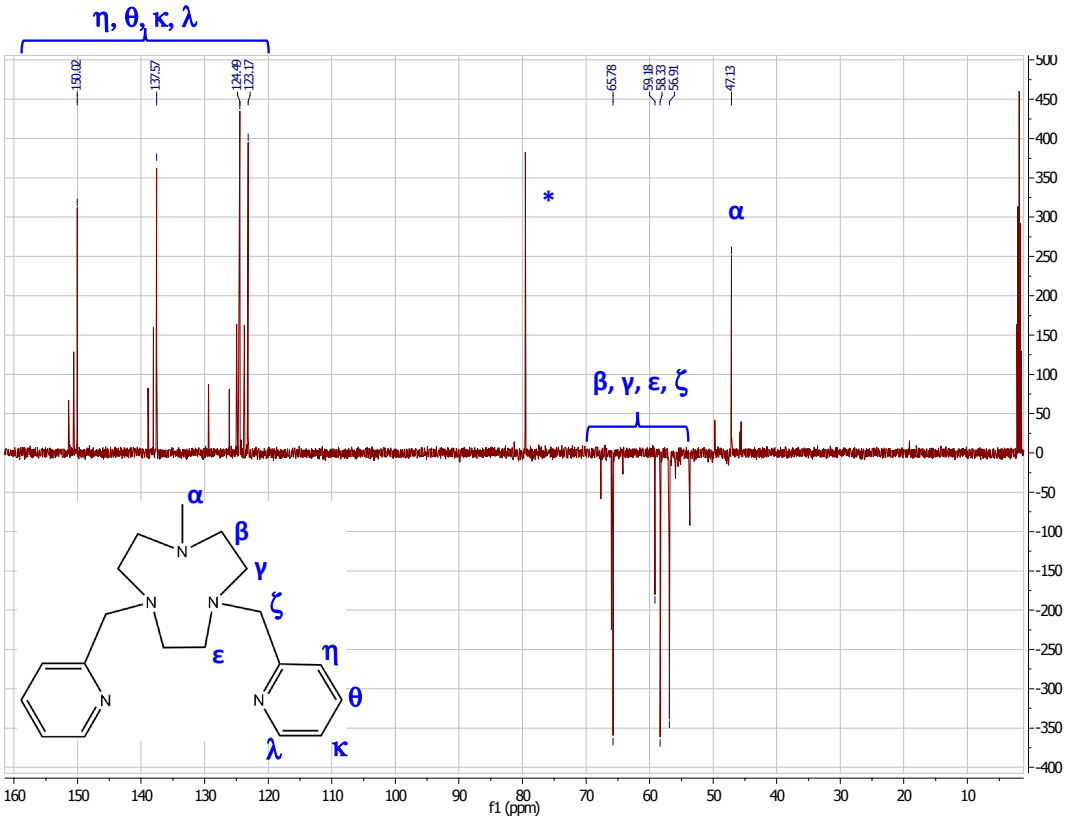

Figure S4. GC chromatogram of $(CH_2Py)_2Me[9]aneN_3$. RTx-5 Amine S-77 column 15 m long and 0.25 mm diameter, FID detector, temperature ramp from 70ºC to 300ºC (8ºC per minute), gas carrier H_2 0.42 bar, 1.7 mL/min, 1.0 µL inyection volume: 23.07 min retention time, 90.2% purity.

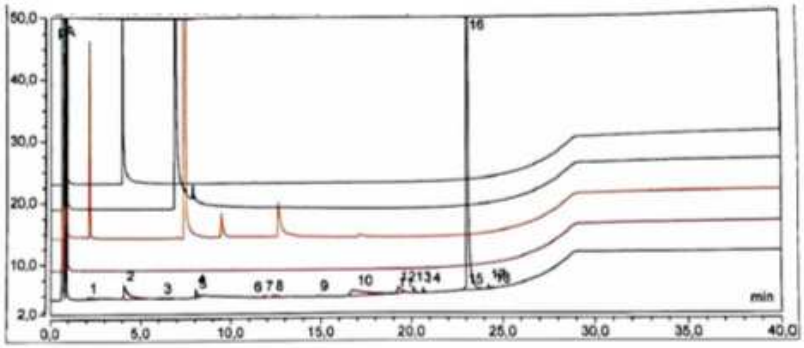

Picolyl chloride
$Me[9]aneN_3$
Orthoamide
$CHCl_3$
Sample

No.	Ret.Time min	Peak Name	Area pA*min	Rel.Area %
1	2,05		0,068	0,309
2	4,10		0,565	2,565
3	6,16		0,078	0,353
4	8,04		0,077	0,352
5	8,11		0,063	0,286
6	11,16		0,010	0,046
7	11,80		0,034	0,154
8	12,36		0,068	0,307
9	14,84		0,009	0,041
10	16,87		0,746	3,391
11	19,13		0,005	0,023
12	19,25		0,216	0,981
13	20,10		0,076	0,346
14	20,82		0,055	0,250
15	22,97		0,024	0,111
16	23,07		19,855	90,217
17	24,21		0,048	0,220
18	24,45		0,011	0,049
Total:				**100,000**

$(CH_2Py)_2Me[9]aneN_3$

Characterization of $[Fe((CH_2Py)_2Me[9]aneN_3)(NO)](BF_4)_2$

Figure S5. ESI-MS spectrum of [**1-NO**]$^{2+}$ in water/acetonitrile. Top: positive mode. Bottom: negative mode.

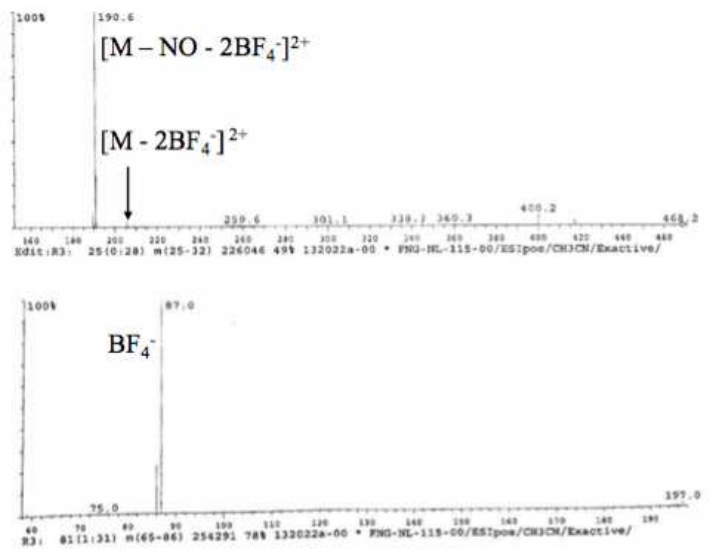

Table S1. Crystallographic Data

	$[Fe((CH_2)Py)_2Me[9]aneN_3)(NO)](BF_4)_2$
formula	$C_{19}H_{27}B_2F_8N_6OFe$
Mr	584.92
crystal system	orthorhombic
space group	$P2_12_12_1$
a / Å	10.4169(14)
b / Å	10.7244(15)
c / Å	21.330(3)
V / Å^3	2382.9(6)
Z	4
Dcalc/Mg.m^{-3}	1.630
T/K	100(2)
μ/mm-1	0.722
data/parameters	6951 / 367
θ range/deg	2.726 – 29.999
collected/unique refl.	64437 / 6951
R1, wR2 (I>2σ(I))a	0.0535 , 0.1475
R1, wR2 (all data)	0.0614 , 0.1555
GoF (F2)	1.056
Absolute Structure Parameter	0.017(5)

Table S2. Selected bond lengths and angles of [**1-NO**]$(BF_4)_2$.

	[**1-NO**]$(BF_4)_2$
Distances / Å	
Fe-N(1)	1.731(3)
Fe-N(2)	2.096(3)
Fe-N(3)	1.987(3)
Fe-N(4)	2.031(4)
Fe-N(5)	1.992(3)
Fe-N(6)	1.991(4)
N(1)-O(1)	1.143(6)
Angle / º	
N(2)-Fe-N(6)	85.1(2)
N(2)-Fe-N(4)	83.7(2)
N(2)-Fe-N(3)	81.4(1)
N(2)-Fe-N(5)	92.6(1)
N(2)-Fe-N(1)	177.3(2)
N(6)-Fe-N(4)	86.6(2)
N(6)-Fe-N(3)	165.8(2)
N(6)-Fe-N(5)	82.4(2)
N(6)-Fe-N(1)	96.3(2)
N(4)-Fe-N(3)	96.3(2)
N(4)-Fe-N(5)	168.7(2)
N(4)-Fe-N(1)	94.0(2)
N(3)-Fe-N(5)	93.7(1)
N(3)-Fe-N(1)	97.4(2)
N(5)- Fe-N(1)	89.8(2)
Fe-N(1)-O(1)	148.3(4)

Figure S6: Packing in the crystal of [**1-NO**]$(BF_4)_2$.

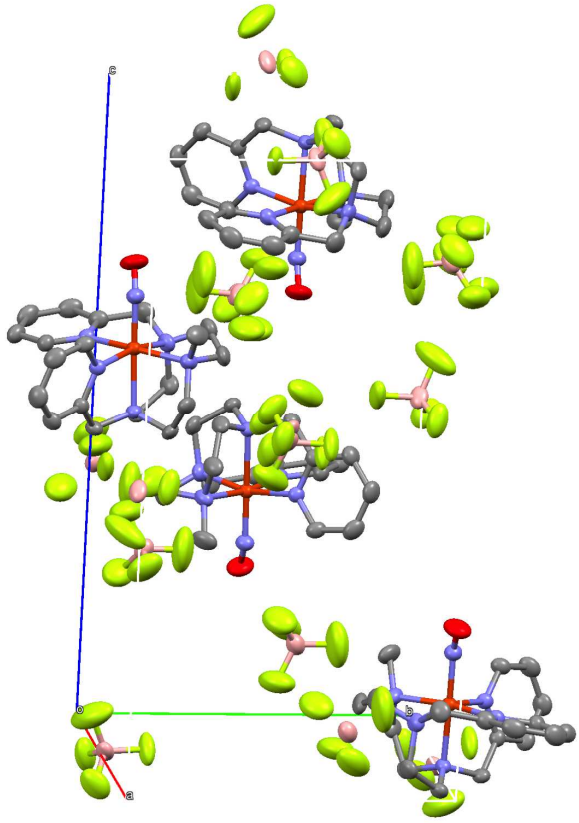

Figure S7: IR spectrum (ATR) of [**1-NO**]$(BF_4)_2$.

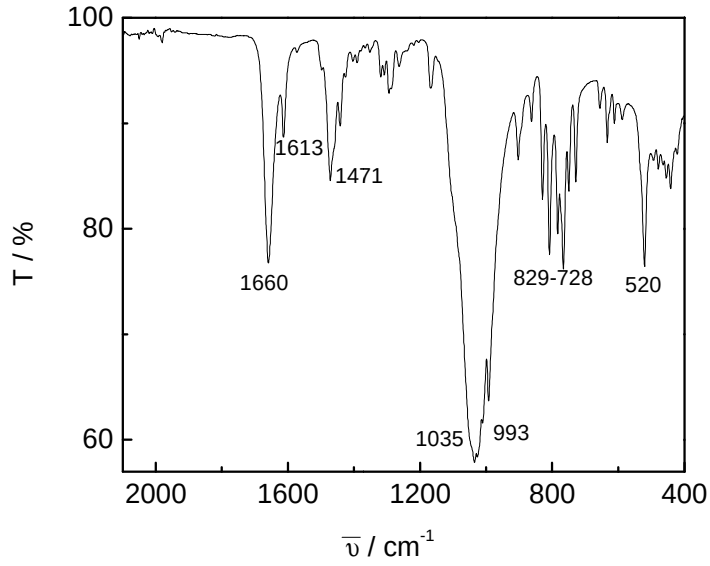

Table S3. UV-Vis spectra maxima of the species $\{FeNO\}^{6/7/8}$ obtained by spectroelectrochemistry of [**1-NO**]$(BF_4)_2$ in CH_3CN/0.1 M $[Bu_4N]PF_6$ at T = (-20±1) ºC in anaerobic conditions (Ar); [a]T = (25±1) ºC.

{FeNO}^{n}, n	**λ_{max} / nm (ε / M^{-1}cm^{-1})**
6	248 (2.6 x 10^4)
7	242 (2.1 x 10^4, 2.0 x 10^4 [a]) 318 (3.0 x 10^3, 3.6 x 10^4 [a]), sh
8	254 (8.6 x 10^3) 398 (3.7 x 10^3), sh 418 (4.3 x 10^3) 536 (1.1 x 10^3)

Figure S8. Spectral changes in the UV-vis spectra of an acetonitrile solution of [**1-NO**]$(BF_4)_2$ interacting with a light source (λ_{irr} = 365 nm) in anaerobic conditions (Ar). Inset: calculated concentration profiles for [**1-NO**]$^{2+}$ (black) and [**1-CH$_3$CN**]$^{2+}$ (red). The estimated ϕ_{NO} is 0.40 mol.einstein^{-1}.

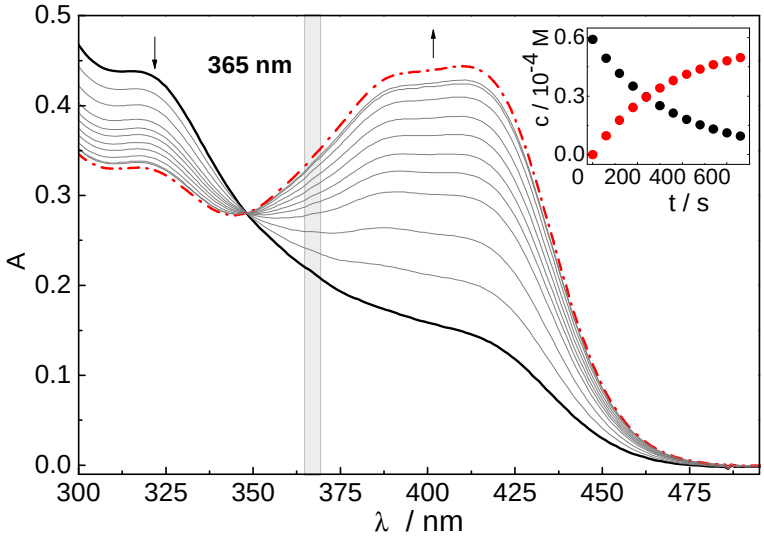

Figure S9. Qualitative detection of NO evolution along the photolysis experiments. A *ca* 1×10^{-6} M solution of metMb (dashed spectrum) at pH = 7.2 (30 mM phosphate buffer) was treated with dithionite under argon to yield Mb, the reduced myoglobin (red spectrum). An argon stream was passed through the irradiated solution of **[1-NO](BF$_4$)$_2$** and collected over the Mb solution. The arrows indicate the spectral changes due to the formation of Mb-NO (λ_{max} = 421nm, Soret band), confirming the photoproduction of NO.

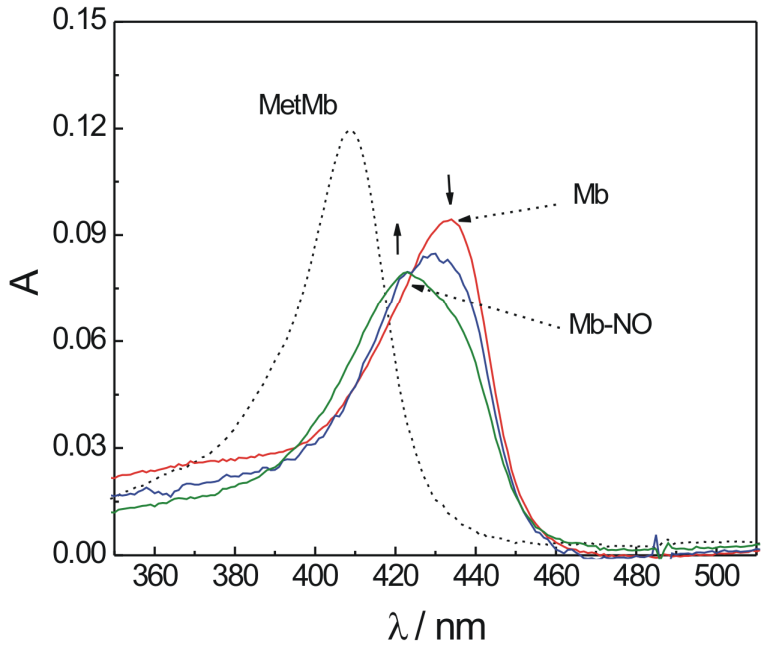

Figure S10. Frontier orbitals computed after a corresponding orbital transformation for the S = 3/2 state of [**1-NO**]$^{2+}$ at the BP86/TZV(P) level of theory.

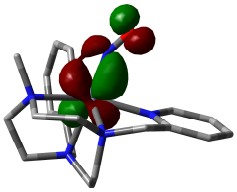

105α

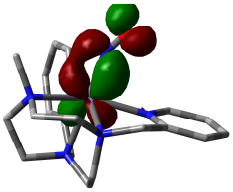

105β

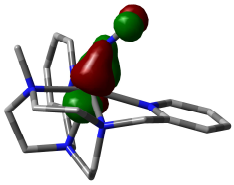

106α

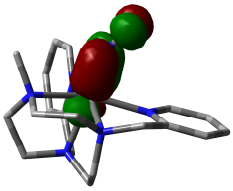

106β

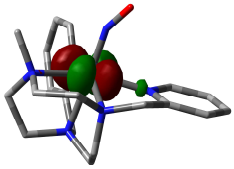

107α

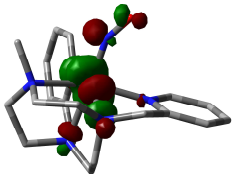

108α

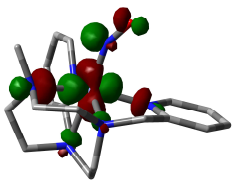

109α

Figure S11. Frontier orbitals computed after a corresponding orbital transformation for the S = 2 state of [**1-AcN**]$^{2+}$ at the BP86/TZV(P) level of theory.

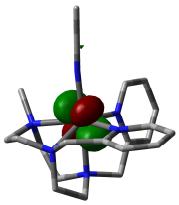

109α

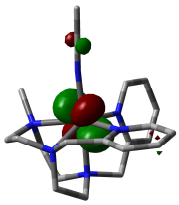

109β

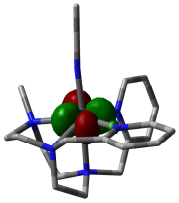

110α

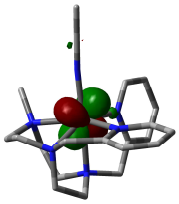

111α

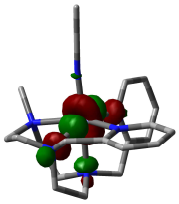

112α

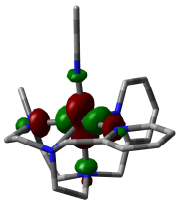

113α